Research Article

SOHAG JOURNAL OF SCIENCES

https://doi.org/10.21608/sjsci.2024.329378.1229

Design, preparation, structural inspection, and biological applications of novel VO^{2+} azomethine complex

Laila H. Abdel-Rahman[1,*], Ayman Nafady[1,2], Ahmed M. Kassem[1], Ahmed M. Abu-Dief [1,3]

[1] Department of Chemistry, Faculty of Science, Sohag University, Sohag, 82524 Egypt
[2] Department of Chemistry, College of Science, King Saud University, Riyadh, Saudi Arabia
[3] Chemistry Department, College of Science, Taibah University, P.O. Box 344, Madinah, Saudi Arabia
[*]*Email: Laila.abdelrahman@science.sohag.edu.eg*

Received: 19th October 2024, **Revised:** 22nd November 2024, **Accepted:** 28th December 2024
Published online: 1st February 2025

Abstract: Schiff base ligand (L) drived from 2-aminobenzothiazole and 4-hydroxybenzaldehyde was used to synthesis of a novel bioactive complex with VO(II) ion. Elemental analysis, molar conductivity, magnetic moment, infrared, ^{1}H NMR, ^{13}C-NMR, and UV-Vis were used to characterize the suggested structure. Spectroscopic and analytical data have led to the proposal of an appropriate geometry for the complex. VO(II) is present in the square pyramidal complex. By applying Job approaches, the complex's formation constant has been established. Additionally, the synthesized Schiff base ligand and its complex have been tested "*in vitro*" for antibacterial activity against three strains of the fungus *A. flavus, C. candidum,* and *F. oxysporum* as well as three bacteria, *Bacillus cereus, Salmonella Typhimurium,* and *E. coli*. It was demonstrated that the complex had more antibacterial action than the ligand. A concentration-dependent effect of the novel compound was seen in the reduction of breast cancer cells' (MCF-7) cell viability. The result is given as an IC50 value, where the VO(II) complex value show the potential anticancer properties of the compound. The compound's antioxidant activity was examined "*in vitro*", and the findings demonstrated the VO(II) complex's valued ability to scavenge free radicals.
Keywords: VO(II) complex; Spectroscopic charachterization; cytotoxicity; anti-pathogenic; DPPH inhibition.

1. Introduction

Cancer is one of the major causes of mortality and morbidity worldwide. One of the most deadly illnesses in the world, cancer is defined by the aggressive and unchecked growth of aberrant cells. It is anticipated that there will be 2,001,140 new cases of cancer and 611,720 cancer-related deaths in the US in 2024. Through 2021, cancer mortality decreased further, preventing almost 4 million lives since 1991 as a result of decreased smoking, early cancer identification, and better adjuvant and metastatic treatment choices. [1]. Benzothiazole represents an entire class of sulphur-containing heterocyclic compounds comprising a benzene ring fused with a thiazole ring. Since the benzothiazole heterosystem has so many uses as phytohormones, antioxidants, electroluminescent devices, vulcanization inducers, and enzyme inhibitors, it is mostly found in natural substances. [2-15].

Schiff bases are excellent nitrogen donor ligands. The capacity of Ligand to generate compounds with transition-metal ions is determined by this various characteristic [16-20]. 2-aminobenzothiazole is an important family of these heterocycles that has garnered a lot of interest because of its several uses as a favored structure in medicinal chemistry and drug development studies. An important 2-aminobenzothiazole-based medication for the deadly neurological illness amyotrophic lateral sclerosis [21]. The metal complex of Schiff bases that is produced from heterocyclic compounds with ligand atoms of nitrogen, sulfur, and/or oxygen is recognized as a basic structural model of more sophisticated biological systems. One of the leading reasons to die in contemporary society is cancer, and the proportion of cancer patients is rising swiftly, demonstrating the importance and broad nature of this health issue [22].

The primary objective of research organizations is the creation and manufacture of new chemotherapy with fewer side effects, since anticancer medicines also exhibit poisoning to healthy cells. The utilitarian characteristics of these complexes have gotten a lot of attention because of their various applications, involving analytical chemistry, electrochemistry, food, agrochemical, pharmaceutical, and dye industries, and biological fields, because of their structure flexibility, sensitivity well selectivity towards a multiplicity of micro-organisms. This has led to the synthesis of several complexes with various main ions and ligands. Indeed, these complicated compounds have demonstrated remarkable efficacy against several cancer cell types. Given the foregoing, the current study uses a green mechanochemical approach to synthesize the V (II) complex obtained from 2 aminobenzothiazole Schiff base and investigate its antibacterial and antifungal properties [23].

The advancement of spectral approaches has made it possible to elucidate the mechanics behind biological events currently. It is being shown that some processes in living things occur on Schiff bases, which interact with free metal ions and neutralize the damaging impacts of aldehyde and

amine components. The reason Schiff bases are referred to as auxiliary ligands is that they alter the reactivity and structure of the transition metal ion at the complex's core; in contrast to reactive ligands, they do not themselves experience irreversible changes. [24]. These are due to their most significant medicinal uses: antibacterial [25, 26] and antifungal [27] (including anti-yeast) activity, antiviral [28, 29], antitumor [30, 31], antiinflammatory [32], antipyretic, antimalarial [33], anticancer [34–36], anesthetic, oxytocin imitating. It has been demonstrated that these chemicals' imine group is necessary for their biological effects [37- 39]. VO (II) complex has been illustrated to have biological, catalytic, and optoelectronic utilizes [40]. The VO (II) azomethine complex will be investigated for its cytotoxic effects against cancer cell lines. The novelty lies in exploring its mechanism of action, such as inducing apoptosis through DNA interaction or inhibition of enzymes critical for cancer cell proliferation. The distinct electronic properties of VO (II) might lead to unique interactions with biomolecules, differentiating its activity from conventional vanadium-based complexes.

These considerations, together with our efforts to create metal-based medicinal medicines, lead us to plan a systematic study of the synthesis, spectroscopic analysis, and scientific jobs of new metallo-complex in transition that include the (L) ligand 2-aminobenzothiazole with 4-hydroxybenzaldehyde, in addition to chemical studies, (MS) analytical techniques, infrared radiation (IR), ^{1}HNMR, ^{13}C-NMR, and ultraviolet-visible (UV-vis) spectroscopies. It is also necessary to develop novel sensitizing substances that can specifically raise the detrimental effect of chemotherapy medications on cancerous cells. Furthermore,"*in vitro*"assays was performed for complex to examine it's antibacterial, antioxidant and anticancer, which measure their effective scope in bioinorganic chemistry.

2. Materials and methods

2.1. Reagents, Instrumentation and methods

All of the solvents and reagents used in this investigation were full reagent assessments, and they were used just as provided, without any further purification procedures. Starting materials such 2-Aminobenzothiazole, 97% (Across Belgium) with 4-hydroxybenzaldehyde, 98% (Across Belgium) in addition to solvents that are organic, like Ethyl alcohol, 99.9%, DMSO (99%) and metal salts such as Vanadium acetylacetonate(VO($C_5H_7O_2$)$_3$, 99%.

2.2. preparation of ligands

2.2.1. Synthesis of 4-(Benzothiazol-2-yliminomethyl)-phenol ligand (L)

The investigated azomethine ligand was synthesised as follow: reaction of 2-aminobenzothiazole (5 mmol, 0.75 g in 10 ml ethanol) and 4-hydroxybenzaldehyde (5 mmol, 0.616 g in 10 ml ethanol). After three hours of reflux heating, stirring, and subsequent evaporation, the ligand (L) was obtained as shown in **Scheme 1**.

L color: yellow, molecular formula $C_{14}H_{10}N_2OS$ (254.311) mp: 228 ºC. Anal. Calcd (%): C, 66.12, H, 3.96, N, 11.015; found (%): C, 66.17, H, 3.91, N, 10.95. Solubility: EtOH. IR: 3056 (OH), 1275 (C-S), 1642 (-C=N). ^{1}HNMR δ-DMSO-d_6: 9.8 ppm (OH proton), 8.07-6.99 (phenyl ring), 9.07 (H-C=N azomethine proton). ^{13}C NMR δ-DMSO d_6: 173 ppm, 166.86 ppm (-C=NH), 135-116 ppm (Phenyl ring) (**Figs. 2, and S2**).

2.2.2. Preparation of VO[4-(Benzothiazol-2-yliminomethyl)-phenol] complex

The ligand (L) was produced and weighed (2 mmol, 0.651 g). It was then diluted in 10 mL of ethanol before being added one at each step to 1 mmol of VO $(C_5H_7O_2)_3$ vanadium acetylacetonate (0.265 g). After five hours of reflux heating, stirring, and subsequent evaporation, the product complex was concentrated. The crystalline complex was separated by filtration, and after that, it was dried in desiccators and cleaned with ethanol. The resulting complex is LV (**Scheme 1**).

[**LV**] (Deep brown): Molecular formula $C_{24}H_{26}N_2VO_7S$ (537.4849), mp: 260ºC. Anal. Calcd (%): C, 53.63, H, 4.88, N, 5.21, found (%): C, 53.67, H, 4.93, N, 5.27: solubility: ethanol:IR: 3382 (OH), 1273 (C-S), 1598 (C=N), 433 (M─N) and 548 (M─O).

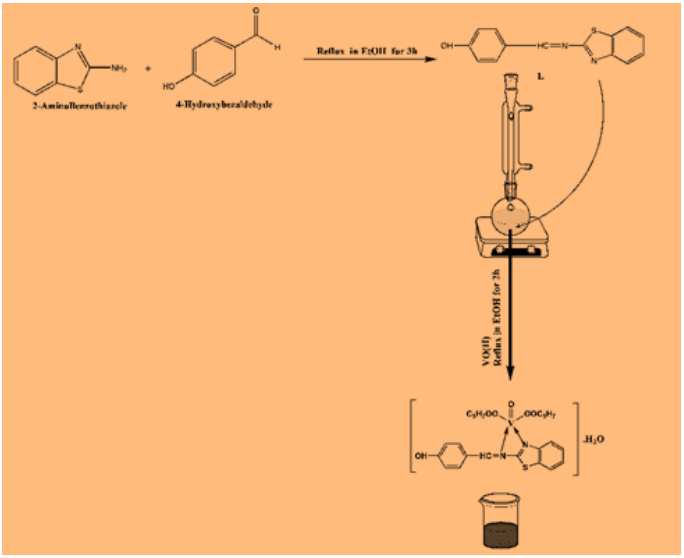

Scheme1: Synthetic pathway for preparation of L ligand complex.

2.3. Estimation of Stoichiometry of Complex

The exact stoichiometry in solution of the produced complex was estimated using the continuous variation technique and the molar ratio [41]. Product of ligand and salt of metal was added, mixed, and left to balance. Plotting the intensity of absorption at λ_{max} versus the mole fraction of either ligand or the metal ion was done for all of the solutions.

2.4. Formation constant of complex in solution

Using spectrophotometry, the formation constants (K_f) of complex was found for frishely prepared concentrations of metal ion and ligand solutions in accordance with Job technique. This by using the subsequent formula [42].

$$K_f = \frac{A/Am}{C(1 - A/Am)^2} \quad (1)$$

For 1M:1L

Whereas, [C] = initial metal concentration determined by molarity.

[A_m]= denotes the complexation method's highest level of absorption at fulfillment.
[A] = denotes a number of absorbance points chosen from each side of the peak.
Furthermore, the alteration in complex free energy, or ΔG, is calculated using this connection: -RT Ln K_f = ΔG.
Where T is temperature in kelvin, Kf is formation constant, and R is the gas constant.

2.5. Biological investigation

2.5.1. Antimicrobial assessment:

Applying the diffusion technique of well and the minimum inhibitory concentration (MIC), the antibacterial abilities of the (L) ligand and its complex was assessed against a variety of *Bacillus cereus, Salmonella Typhimurium and E. coli*. The pair of standards used to measure efficiency were the antifungal drug fluconazole and the antibacterial drug ofloxacin [43]. The investigated compounds were dissolved in DMSO at different concentrations between ten and twenty mg/L. Using this technique, inhibitory zone diameters and minimum inhibitory concentrations (MIC, mg/mL) are estimated. All composites exhibited intriguing antibacterial properties. Every metal ion has a valence band that crosses over into the ligand orbital. Enhanced activity promotes complex lipophilicity accruing to p-electron delocalization in the chelate ring. Under certain circumstance, this enhanced lipophilicity results in the malfunction of the cell's permeability barrier [44, 45]. This notion is supported by a broad inhibitory region, a considerable portion of the activity index, and restricted MIC values. The variation in the activity of different complex against tested organisms is likely due to either the bacteria' cells' resistance or the variations in microbial cells' ribosomes [46]. The capacity for antibacterial activity is greatly influenced by variables including coordination sites, hydrophobicity, dipole moment, complicated geometry, bond length, and concentration [47]. Applying the following connection, the effectiveness index of the ligand L that was examined as well as its complex was calculated.

$$\text{Activity index} = \frac{\text{Inhibitionzoneof compound (mm)}}{\text{Inhibitionzoneof thestandarddrug (mm)}} * 100$$

2.5.1.1. Dedication of MIC for the compounds under Prosecution:

Determine the minimum restricted concentration for each chemical throughout the examination to foresee the development of microorganisms at the scale of the microscopic. The attack was timed exactly with the least concentration of the medicine under examination, which was clearly effective in stopping the development of bacteria. The chosen derivative was produced in Mueller-Hinton broth that had been sterilized, with different concentrations of 20, 10, 9, 8, 7, 6, 5, 4, 3, 2, and 1 µg mL^{-1}. Bacterial abundance was adjusted to 0.5 McFarland in sterile water containing peptone. Afterwards, 1 mL of suspension (0.5 McFarland) was added to each sample. The culture was incubated at 38 ◦C for 47 hours. Specimen from nozzle was inspected after incubation to make sure there was no evident evidence of bacterial proliferation. It was then placed on culture media for a period of 24 to 72 hours [48].

2.5.2. Anti-cancer activity

Different human cancer cell lines—HCT-116, which is a type of colon cancer; HepG-2, a type of hepatic cellular carcinoma; and MCF-7, a type of breast cancer—were used to test compound anticancer potential. The cells were allowed to interact with the supports for 24 hours at 37 °C. A spectrophotometric assessment of the unit decrease in growth was conducted using sulforhodamine B (SRB) [49]. The results of the inhibitory concentration percent IC was determined.

$$\text{(IC) \% (\%)} = \frac{\text{ControlOD} - \text{CompoundOD}}{\text{ControlOD}} \text{ x } 100$$

Around 564 nm, the optical density (OD) of each well was roughly estimated.

2.5.3. Antioxidant activity by the DPPH method

The L ligand and its complex was evaluated for their antioxidant properties, mixed into an ethanol solvent containing 100 M DPPH radical after being repeatedly diluted (20, 40, 80, 160, and 320 µM). After stirring the mixture, let it sit at 35 °C for 30 minutes. A UV-vis spectroscopy was used to monitor the drop in DPPH intensity at 517 nm. The same investigation was conducted without the complex as a control in order to calculate the IC_{50} and (%) of free radical scavenging behavior. The proportion of the chemicals that were blocked was calculated using the method [50-52]:

$$\textbf{DDPH inhibition effect (\%)} = \frac{\textbf{Ao}-\textbf{As}}{\textbf{Ao}} \textbf{x100} \qquad \textbf{(2)}$$

Where [As] and [Ao] stand for the sample's and control's respective potentials.

3. Results and Discussion:

3.1. General properties

The ligand (L) interacts with vanadium acetylacetonate to create a fresh solid complex in alcoholic. The colorful solid complex was characterized by elemental analysis, molar conductivity, magnetic, infrared, and ultraviolet-visible spectra.

3.2. IR-spectral data

To verify the production of ligand and compound of metal, the IR distributions of L and its complex are discussed. (**Fig. S1 and Table1**). Particularly notable peaks that have altered or recently emerged are investigated because some peaks are of importance based on a comparison of their FT-IR ranges. The OH group and CH=N groups of the (L) ligand exhibit a peak at 3056 cm^{-1}. At 1642 cm^{-1}, display a peak. The spectra of (LV) shift this band to 3382 cm^{-1}. The spectra of (LV) show that this band shifts to 1598 cm^{-1} upon complexation. With FT-IR The band at 960 cm^{-1} in the spectroscopy of the VO (II) complex under investigation was ascribed to VO (II) vibration in the monomeric complex. This band's shift is a clear sign that the nitrogen atoms in azomethine are involved in the creation of the complex [53]. This is supported by the appearance of bands at 548 cm^{-1} corresponding to the stretching vibration of M—O bond in VL complex. The group's stretching vibration may be the cause of the absorption band at 1285 cm^{-1} in the Schiff base spectrum's low frequency area. (C—S). There is no notable change in the position of this peak in (LV) complex which

imply non-involvement of sulfur atom in coordination with metal.

Table 1:- The synthesized L ligand, together with its complex, analysis of Compound , melting points, decomposition temperatures, conductivities, and distinctive IR bands.

Compound	formula	Color	m.p (°C)	μ_{eff} (B.M.)	(Ω^{-1} cm^2 mol^{-1}) Λm	Analysis : found (calcd)			IR, Cm^{-1}				
						C (%)	H (%)	N (%)	(OH)/H2O	St (-CH=N)	ph (C-O)	(M-O)	(M-N)
L	$C_{14}H_{10}N_2OS$ (254.3114)	yellow	228	-	-	10.95 (11.015)	5.27 (5.21)	10.95 (11.015)	3056	1642	(C-S) 1285	-	-
LV	$C_{24}H_{26}N_2VO_7S$ (537.4849)	Deep Brown	260	1.79	11.54	3.91 (3.96)	4.93 (4.88)	3.91 (3.96)	3382	1598	1250	548	433

3.3 ^{1}H NMR and ^{13}C NMR Spectra

The Schiff base ligand (L) ^{1}H NMR (**Fig. 1**) revealed a singlet signal at 9.8 ppm that was identified as an OH proton. The ^{1}H NMR spectra of the Ligand gives demonstrated signals between 6.99 and 8.07 ppm that was identified as phenyl rings. Azomethine proton (H-C=N) was detected at 9.07 ppm as an individual [54].

In ^{13}CNMR spectra (**Fig. S2**), at 173 ppm, 166.86ppm The -C=NH group's extremely unusual spectral fingerprint was discovered. The findings at (152–116) ppm also most certainly matched the phenyl ring The L ligand's 200–800 nm UV–visible spectra in DMF medium demonstrates It is possible to characterize two bands at 218 and 362 nm as the OH, C=N, and NH groups' π → π*, and n → π* transitional periods[55] (**Fig. 2 and Table S1**). Together with the electrical alterations that take place within the metal orbitals, the binding of metallic ions to the ligand results in significant alterations to the molecule itself, indicating the complex constructing. Current bands were found in complex about 270–361 nm, and it was linked to the ligand–metal transfer of charges. In addition, square-pyramidal geometry was demonstrated by the d → d make shift in the (LV) complicated which was planned at 361 nm.

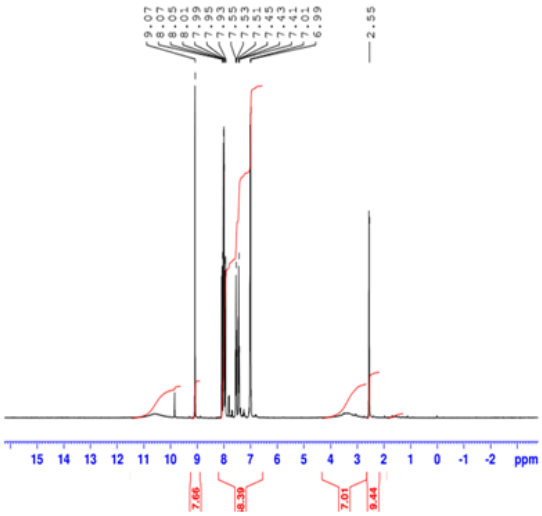

Fig. 1:- The ^{1}HNMR Spectrum of (L).

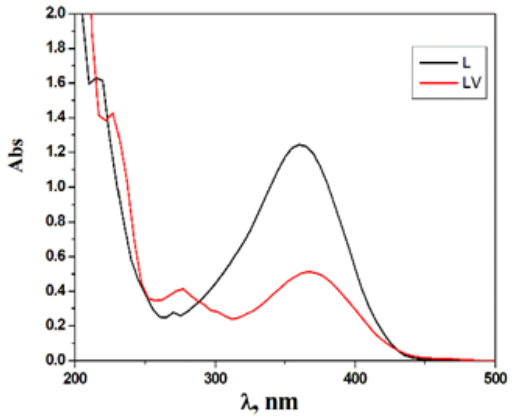

Fig. 2: L-ligand and LV complex (10^{-3} M) molecular spectra in DMF at 298 K.

3.5. Elemental analyses and electrical conductivity measurements

The VO(II) complex seemed to has a 1:1 molar ratio (**Table 2**). Because the compound structure doesn't contain any counterions, it is not electrolytes. For LV complex, the molar conductivity ratio is 11.54 (**Table 1**) [56].

3.5. Magnetic Measurements:

The corresponding magnetic value of VL complex was 1.79 B.M. which is consistent with the d^1 configuration in a square-pyramidal geometry [57].

3.6. Mass Spectrometry

The LV complex mass spectra is shown in (**Fig. 3**). It is widely acknowledged that the complex had a peak of molecular ions at 537.82 amu with a level intensity of 21.81% for the [V ($C_{24}H_{26}N_2O_7S$)] complex. (**Scheme 2**) consisted of nine sections that examined the extra fragmentation ions that were found; Beaks indicate the intensity of the ionic species at m/z 519.48 , 503.48 , 487.48 , 404.43 , 388.43 , 305.38 , 172.08 , 121.08 , 94.06 and 78 culminating in the final dissociation of the benzene, the prognostic molecular weight (537.48 amu). The mass spectrum data supports the inference made from the microanalytical and molar conductivity readings.

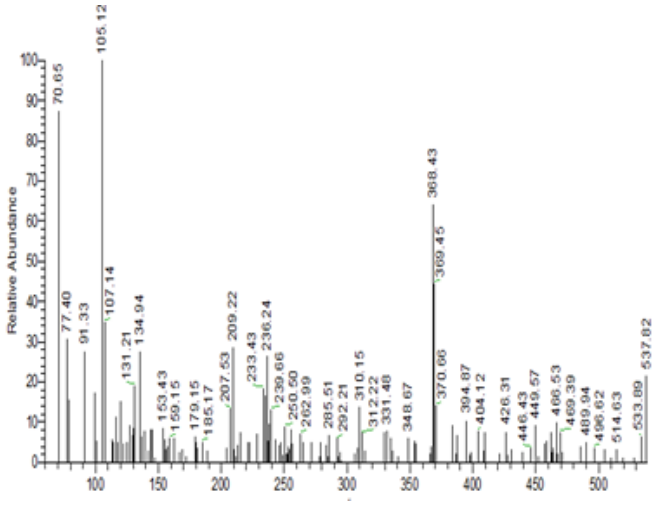

Fig. 3: Mass spectrometry of [V ($C_{24}H_{26}N_2O_7S$)] complex

3.7. Complex stoichiometry, formation constant and solution's pH pattern

The complex's equilibrium concentration produced by the mixture between (L) and the metallic salt VO(II) was determined with Job's and molar ratio calculation techniques. The formation constants (Kf) of the generated complex was determined from spectroscopy measurements through the continuous variation method (**Figs. 4, S3, and Table2**). Complex seem more consistent through pH =4-10 to anticipate the stability of complex under various application conditions in an extensive variety of acidity (Fig. 5). The chelation effect significantly enhances the stability of the VO(II) complex, making it less prone to hydrolysis or ligand displacement in aqueous and biological environments. Moreover, the highly stable LV complex tends to exhibit enhanced selectivity and reduced toxicity. The produced K_f readings demonstrate the constructed compound remarkable stability. Additionally, the complex Gibbs free energy and stability constant value was calculated. The value of the forward and inverse signs of the Gibbs free energy was also assessed in order to evaluate the level of compound formation spontaneity **[58].**

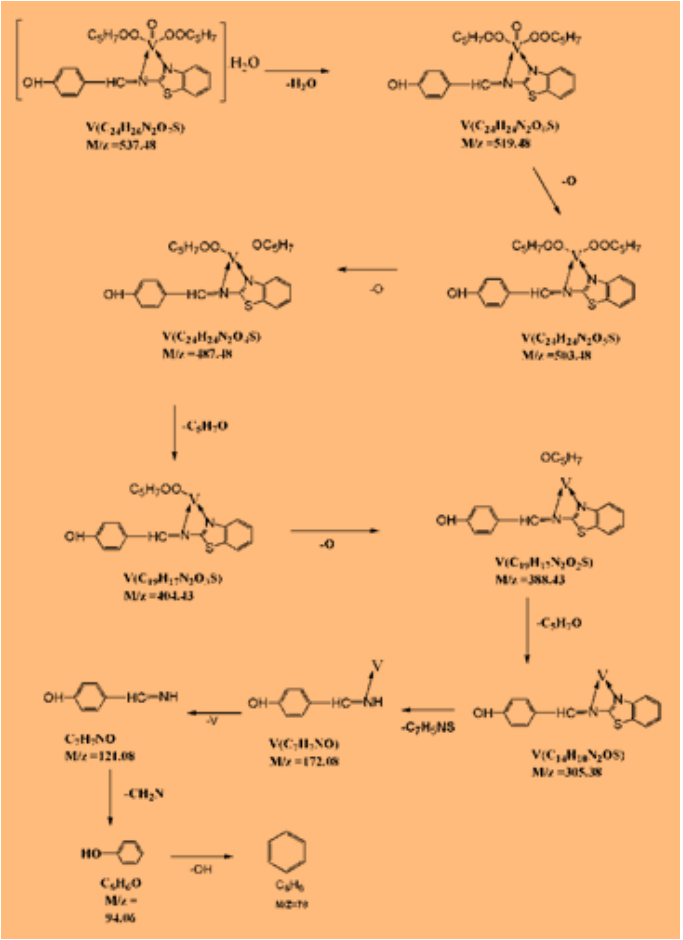

Scheme 2: Route of LV complex fragmentation. The exact masses and chemical formulae of the particles are shown beneath each structure.

Table 2: Formation constant (Kf), stability constant (pK), and Gibbs free energy (G*) value of the synthetic complex at 298 K.

complex	Type of complex	K_F	Log K_F	ΔG ($KJmol^{-1}$)
LV	1:1	4.67×10^3	3.67	**- 20.93**

3.8.The metal complex that the L ligand forms and their bioactivity

3.8.1. Antimicrobial assessment

The ability of the producing L and its metal complex to combat specific strains of bacteria was carefully examined. (*Bacillus cereus, Salmonella Typhimurium and E. coli)* and fungi (*A. flavus, C. candidum, and F. oxysporum*) by indicating the minimum tested microorganism concentration (MIC) in the inhibitory zone (**Table 3, S2 and Fig. 6**). LV complex shows

potent antimicrobial activity compared to its ligand. The enhancement in the antibacterial activity of the investigated VL complex as compared to L ligand can be supported by Overtone's concepts. The chelation process lowers the metal atom's polarity significantly by positive charge transfer with the donating groups and possible π-electron delocalization throughout the whole chelation ring. The core atom becomes more lipophilic due to the chelation process ring; this makes it easier for it to get through the cell membrane's fatty layer [59].

Strong cell surface toxic effects, structural specificity, and a large redox potential (as reported by redox characteristics) that may impact the biomolecules inside the cell or on the outermost layer of the cell might be the building blocks for the increased antimicrobial activity of complicated metal [59]. Small MIC values, the important limiting area, and a sizable chunk of the activity index all corroborate this assessment. This might be related to the contribution of the positive center (metal), which studies how to work with biological processes and regulate cell division. Also, the argument around the chelation hypothesis focuses on how donor locations lower substance toxicity in complex to a level that is safe if they only partially share a metal positive charge. A compound is therefore favored in the medicinal sector over organic or metal salt that is not bonded. Applying the following connection, the strength of the ligand's index (L) that was examined as well as its complex was calculated (**Table S3**):

$$\text{Activity index} = \frac{\text{Inhibitionzoneof compound (mm)}}{\text{Inhibitionzoneof thestandarddrug (mm)}} * 100$$

The MICs of this drug against the *Bacillus cereus* bacteria was higher than those of other substances. Fungus *candida*, in that order, is the smallest. The ligand's and its complex's bioactivity is discovered to be in the sequence that follows: LV > L. The type of metal ions and the bacteria's cell membranes are the reasons for the variations in antimicrobial action.

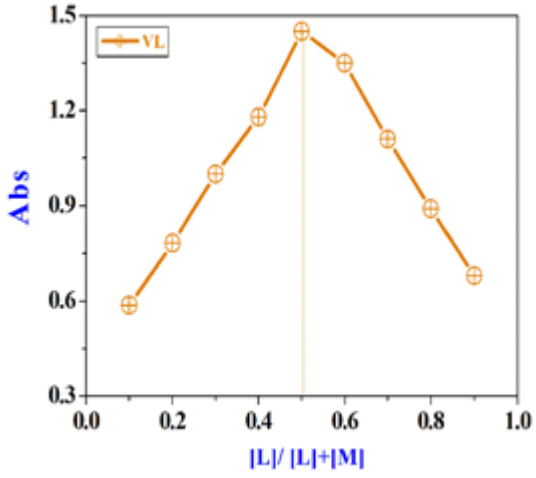

Fig. 4: Job's technique curve for the metal complex in aqueous-ethanol at 298 K

The differences in metal complex action against different bacteria are due to differences in the ribosomes of the microbial cells or the impermeability of the microbes' cells. The reduced activity of complexes relative to others could be due to limited lipid solubility, preventing the metal ion from reaching the cell wall's favorable site of action and interfering with normal cell activity. A comparison of anti-bacterial activity of the inspected compounds with other compounds in literature were reported in Table S2[60].

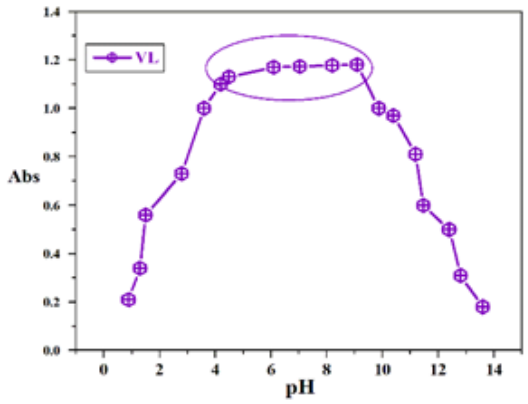

Fig. 5: Impact of pH on the LV complex at 25 °C in aqueous-ethanol media

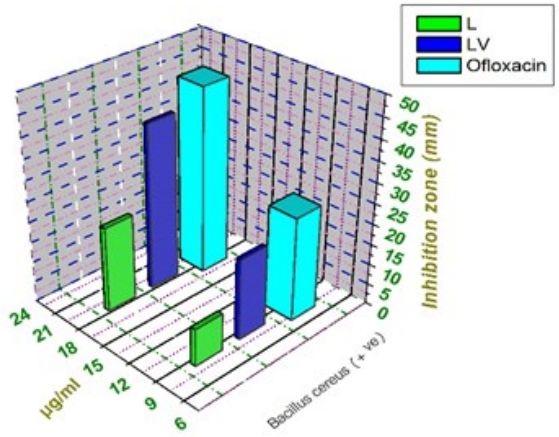

Fig. 6: Chart of antimicrobial for L and LV complex *Bacillus cereus* (+ve).

3.8.2. Anti-cancer activity

Hep-G2, HCT-116, and MCF-7 are three commonly used human cancer cell lines in biomedical research, particularly for studying the cytotoxic effects of new compounds, such as metal complexes, nanoparticles, and synthetic drugs. Each of these cell lines represents a different type of cancer and has distinct biological characteristics, which makes them suitable for various aspects of cancer research. The synthesized substances' cytotoxic activity (IC_{50}) against colon cancer cells (HCT-116 cell line), (HepG-2), and (MCF-7). The median ant proliferative intensity (IC_{50}), which required that the compound have a 50% cytotoxic effect after having been exposed to them for 48 hours, was employed to measure the cell killing capacity of the drugs under research. The computed IC_{50} values highlight that the metal complex has a greater impact than the (L) ligand when it is used lonely This finding demonstrated that the primary mechanism for this complex action, as determined by Tweedy's chelation hypothesis, was the (L) ligand's chelation with the metallic ions V. The harmful effect on cells of the complex is dependent on the metallic ions'

makeup and the kind of ligand. A broad spectrum of pharmacological characteristics has been exhibited by the benzothiazole nucleus in various modifications, including anticancer activities [61]. Because of their unique accuracy in terms of reactivity, redox activity, and coordination patterns, metals are important for a variety of cellular metabolic activities. The metal has the power to produce reactive oxygen species ROS, whish is main for preserve the redox equilibrium inside cell, for the metabolism of cell and for the connecting of cell division, reduplication, and demise. The arrangement is shown by the cytotoxicity that the L ligand and its derivatives may produce in the following cancer cell lines: Hep-G2, HCT-116, and MCF-7: MCF7 > Hep-G2 > HCT116 (**Fig. 7** and **Table S4**). A comparison of anti-cancer activity of the inspected compounds with other related studies were reported in Table S5 [62, 63].

Findings on antimicrobial and anticancer activities of the investigated compounds have significant implications for real-world applications as follow:

1. **Cancer Therapies**: Identifying compounds with selective toxicity against cancer cells can lead to the development of novel chemotherapeutic agents with reduced side effects. Understanding mechanisms like ROS generation or apoptosis induction enhances targeted drug design.
2. **Antimicrobial Treatments**: Novel materials addressing resistance in gram-positive and gram-negative bacteria can offer solutions for multidrug-resistant pathogens, impacting clinical and environmental disinfection applications.

Both fields contribute to advancing precision medicine and global health.

Table 3: Minimum inhibition zone (MIC) for antimicrobial assay of the ligand and its complex.

	bacteria				*fungi*		
compounds	*S. Typhimurium*	*E. Coli (-ve)*	*B. Cereus (+ve)*	*A. Flavus*	*G. Candidum*	*F. Oxysporum*
L	*7.50*	*8.00*	*7.00*	*7.75*	*6.00*	*7.50*
LV	*5.50*	*5.75*	*4.25*	*5.50*	*4.25*	*6.00*
Ofloxacin	*2.75*	*3.25*	*1.75*	-	-	-
Fluconazol	-	-	-	*3.00*	*2.25*	*2.75*

3.8.3 Antioxidant activity

In addition to the aging process, numerous diseases in people are developed as a result of free radical oxidative processes. Various quantities of the L, VO(II) complex of metal with DPPH was used in the antioxidant test inquiry, along with ascorbic acid (vitamin C) as benchmarks. The find corroborated the hypothesis that the complex produced has antioxidant effects against DPPH free radicals comparable to those of regular vitamin C [64]. To assess the effectiveness of antioxidants, complex at different concentrations (10, 25, 50, 100, and 150 µg mL^{-1}) were created, and L-ascorbic acid was used again as a reference for efficiency similarity. Given that its scavenging capacity of DPPH is much greater than that of the free ligand (L), this complex is in contrast, a far stronger and more effective antioxidant and free radical scavenger. The (L) ligand had only moderate antioxidant activity, but the combined forms of V exhibit more antioxidant activity than the ligand. As can be observed (Figure 8 and Table S5), the findings explain the LV complex has the smallest antioxidant efficacy with an IC_{50} of 35.1 µg/mL. The order can be given as LV > L > vitamin C with IC_{50} values as 35.1 > 56.35 > 60.55 µM. The molecules that supply the specimens with their oxidizing potential include those that are capable of contributing just one hydrogen atom to break the chain of free radicals [64].

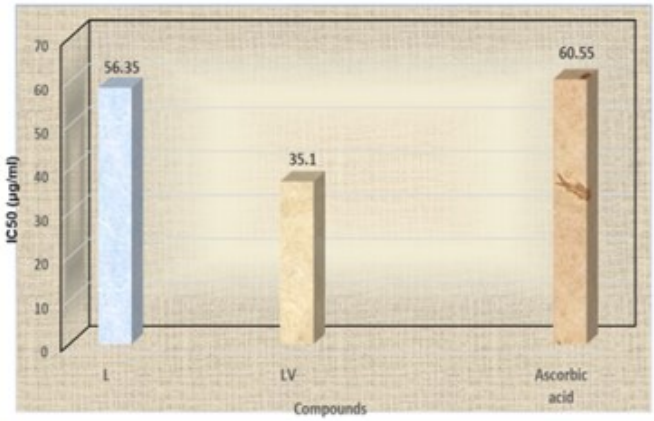

Fig. 8: The antioxidants behavior of compounds.

4. Conclusion

The study on the design, preparation, structural inspection, and biological applications of novel VO(II) azomethine complex highlights several key findings:

i. The novel VO(II) azomethine complexes were successfully synthesized using a Schiff base reaction between a vanadyl ion VO(II) and an azomethine ligand. The synthesis process was optimized to yield stable complexes.

ii. Comprehensive structural analyses, including spectroscopic techniques such as UV-Vis, FT-IR, NMR, and mass spectra, confirmed the formation of the VO(II) azomethine complex. The data indicated a coordination environment where the vanadyl ion was chelated by the azomethine ligand, resulting in a stable square-pyramidal geometry.

iii. Comprehensive structural analyses, including spectroscopic techniques such as UV-Vis, FT-IR, NMR, and mass spectra, confirmed the formation of the VO(II) azomethine complex. The data indicated a coordination environment where the vanadyl ion was chelated by the azomethine ligand, resulting in a stable square-pyramidal

geometry.

iv. Comprehensive structural analyses, including spectroscopic techniques such as UV-Vis, FT-IR, NMR, and mass spectra, confirmed the formation of the VO(II) azomethine complex. The data indicated a coordination environment where the vanadyl ion was chelated by the azomethine ligand, resulting in a stable square-pyramidal geometry.

v. Comprehensive structural analyses, including spectroscopic techniques such as UV-Vis, FT-IR, NMR, and mass spectra, confirmed the formation of the VO(II) azomethine complex. The data indicated a coordination environment where the vanadyl ion was chelated by the azomethine ligand, resulting in a stable square-pyramidal geometry.

vi. The synthesized VO(II) azomethine complex demonstrated promising biological activities. It exhibited notable antioxidant and antimicrobial properties, likely due to the redox-active nature of the vanadyl ion and the electron-donating effects of the azomethine ligand. Additionally, cytotoxicity assays against selected cancer cell lines suggested potential as anticancer agents, warranting further investigation into their mechanism of action.

These features make benzothiazole-based Schiff base promising candidates for developing novel drugs, and advanced functional materials.

CRediT authorship contribution statement:

Conceptualization, Laila H. Abdel-Rahman and Ahmed M. Abu-Dief; methodology, Ahmed M. Kassem; Ahmed M. Abu-Dief software, Ahmed M. Abu-Dief; validation, Ahmed M. Abu-Dief, and Ahmed M. Kassem; formal analysis, Ahmed M. Kassem; Ahmed M. Abu-Dief investigation, Ahmed M. Abu-Dief and Ahmed M. Kassem resources, Laila H. Abdel-Rahman; Ahmed M. Kassem data curation, Ahmed M. Kassem; writing—original draft preparation, Ahmed M. Abu-Dief, Ahmed M. Kassem; writing—review and editing, Laila H. Abdel-Rahman, Ahmed M. Abu-Dief, Ayman Nafady; visualization, Ahmed M. Abu-Dief; supervision, Laila H. Abdel-Rahman; project administration, Laila H. Abdel-Rahman, Ayman Nafady; funding acquisition, Laila H. Abdel-Rahman, Ahmed M. Abu-Dief All authors have read and agreed to the published version of the manuscript.

Data availability statement

The data used to support the findings of this study are available from the corresponding author upon request.

Declaration of competing interest

The authors declare that they have no known competing financial interests or personal relationships that could have appeared to influence the work reported in this paper.

References

[1] H. Sung, J. Ferlay, R.L. Siegel, M. Laversanne, I. Soerjomataram, A. Jemal, F. Bray, *J. Clin*, 3 (2021) 209-249.

[2] K.A. Sumit, Kumar, A. Mishra, An up-to-date review. *Mini. Rev..Med. Chem*., 3 (2021) 314-335.

[3] A.F.M. Mohamed, O.S. El-Sherif, El-Mahdy, H.A. Hozien. *Curr. Org. Chem*, 14(2017) 604-611.

[4] A.S. Ingale, A.P. Dalvi, N.R. Pise, *Commun.*, (2021)1-13.

[5] P.K. Antifungal, Sharma, *Pharm. Lett*., 8(2016)140-142

[6] R.P. Wu, F.L. Hussain, W.M. Ross, B.P. McGeary, *Curr.Org. Chem*., 16 (2012) 1555-1580.

[7] (a) M. Sharma, P.K. Kumar, *Res. Chem.,* 41(2015) 6141-6148; (b) M. Sharma, B.K. Sharma, P.K. Kumar, *Commun. Intermed*., 40 (2010) 2347-2352.

[8] M. Fogla, A.K. Ankodia, V. Sharma, P.K. Kumar. *Res. Chem. Intermed*., 35(2009) 35-41.

[9] C.L. Du, H. Sun, Y. Yang, R. Zhang, W. Wan, J. Chen, Kahramanoglu, I. Zhu, J. Food Qual., (2021) 6631507.

[10] P.K. Sharma, G. Kumar, J. Chem. Pharm. Res., 7(2015)462-473.

[11] P.K. Sharma, A. Amin, M. Kumar, Med. Chem. J., 14(2020)71-82.

[12] M. Sharma, P.K. Amin, A. Kumar,. Med. Chem. J., 14(2020) 49-64.

[13] P.K. Qadir, T. Amin, A. Sarkar, D. Sharma,. Curr. Org. Chem., 25 (2021) 1868-1893.

[14] Sharma, P.K. Makkar, Asian J. Pharm. Clin. Res., 10 (2017) 43-46.

[15] T. Pfeiffer, P. Breith, E. Llibbe, E. Tsumaki, Justus Liebigs Ann. Chem, 503(1933) 84–130.

[16] L. Hunter, J.A. Marriott, J. Chem. Soc., 422 (1937) 2000–2003.

[17] L. Sacconi, M. Ciampolini, F. Maggio, F.P. Cavasini, J. Am. Chem. Soc, 84(1962)3246–3248.

[18] R.H. Holm, K. Swaminathan, Inorg. Chem., 1(1962) 599–607.

[19] G.C. Percy, D.A. Thornton, J. Inorg. Nucl. Chem., 34 (1972) 3357–3367.

[20] G. Bensimon, L. Lacomblez, V. Meininger, A.R.S. Group, N. Engl. J. Med. 330 (1994) 585-591.

[21] B. Cheah, S. Vucic, A. Krishnan, M. Kiernan, Riluzole, Curr. Med. Chem., 17 (2010) 1942-1959.

[22] S. Hosny, M.R. Shehata, S.A. Aly, A.H. Alsehli, M. Salaheldeen, A.M. Abu-Dief, S.M. Abu-El-Wafa, Inorg. Chem. Commun., 160, (2024) 111994.

[23] R.L. Lundgren, M. Stradiotto, J. Wiley, Sons, Ltd.: Chichester, UK; Hoboken, NJ, USA, (2016)1–13.

[24] A.A. Abdel Aziz, A.N.M. Salem, M.A. Sayed, M.M. Aboaly, J. Mol. Struct. 1010 (2012) 130–138.

[25] G. Saravanan, P. Pannerselvam, C.R. Prakash, J. Adv. Pharm. Technol. Res., 1 (2010) 320–325.

[26] O. Gungor, P. Gurkan, J. Mol. Struct, 1074(2014) 62–70.

[27] K.S. Kumar, S. Ganguly, R. Veerasamy, E. DeClercq, Eur. J. Med. Chem., 45(2010)5474–5479.

[28] D. Sriram, P. Yogeswari, N.S. Myneedu, V. Saraswat, Bioorg. Med. Chem. Lett., 16 (2006) 2127–2129.

[29] G. Hu, G. Wang, N. Duan, X. Wen, T. Cao, S. Xie, W.

Huang, Acta Pharm. Sin. B., 2 (2012) 312–317.
[30] N. El-wakiel, M. El-keiy, M. Gaber, Acta. A. mol. Biomol. Spectrosc., 147 (2015) 117–123.
[31] E. Pontiki, D. Hadjipavlou-Litina, A. Chaviara, J. Enzym. Inhib. Med. Chem., 23 (2008) 1011–1017.
[32] P. Rathelot, P. Vanelle, M. Gasquet, F. Delmas, M.P. Crozet, P.J. Timon-David, Maldonado, Eur. J. Med. Chem., 30 (1995) 503–508.
[33] S.M. Bensaber, H. Allafe, N.B. Ermeli, S.B. Mohamed, A.A. Zetrini, S.G. Alsabri, M. Erhuma, A. Hermann, M.I. Jaeda, A.M. Gbaj, Med. Chem. Res. 2 23(2014)5120–5134.
[34] S.B. Desai, P.B. Desai, K.R. Desai, Heterocycl. Commun., 7(2001)83–90.
[35] P. Przybylski, A. Huczynski, K. Pyta, B. Brzezinski, F. Bartl, Curr. Org. Chem., 13 (2009) 124–148.
[36] K.K. Upadhyay, A. Kumar, S. Upadhyay, P.C. Mishra. Journal of Molecular Structure, 873 (2008) 5-16
[37] R. Antony, T. Arun, S.T.D. Manickam, Int. J. Biol. Macromol, 129 (2019) 615-633.
[38] I. Ledeţi, A. Alexa, V. Bercean, G. Vlase, T. Vlase, L.M. Şuta, A. Fuliaş, Int. J. Mol. Sci., 16 (2015) 1711-1727.
[39] L. Wang, Y. Feng, J. Xue, Y.Li, Int. J. Pharm. Technol. Res.1(2008)22.
[40] M. Dehkhodaei, M. Sahihi, H.A. Rudbari, S. Gharaghani, R. Azadbakht, S. Taheri, A. AbbasiKajani, J. Mol. Liq., 248 (2017) 24.
[41] L.H. Abdel-Rahman, A.M. Abu-Dief, R.M. El-Khatib, S.M. Abdel-Fatah, J. Photochem. Photobiol., B 162 (2016) 298.
[42] H.M. Abd El-Lateef, A.M. Abu-Dief, L.H. Abdel-Rahman, E.C. Sañudo, N.A. Alcalde, J. Electroanal. Chem., 743 (2015) 120.
[43] V. Govindaraj, S. Ramanathan, Turk. J. Chem., 38 (2014) 521.
[44] H.W. Horowitz, G.M. Jetzger, Anal. Chem. 35 (1963) 1464.
[45] G.G. Mohamed, M.H. Soliman, Spectrochim. Acta A76 (2010) 341.
[46] S.H. Sumrra, W. Zafar, M. Imran, Z.H. Chohan, J. Coord. Chem., 75 (2022) 293-334.
[47] K. Mounika, A. Pragathi, C. Gyanakumari, Aust. J. Sci. Res., 2 (2010) 513.
[48] S.A. Khan, K. Rizwan, S. Shahid, M.A. Noamaan, T. Rasheed, H. Amjad, Appl. Organomet. Chem., 34 (2020) e5444.
[49] H. Naeimi, Z.S. Nazifi, S.M. Amininezhad, M. Amouheidari, J. Antibiot. 66 (2013) 687–689.
[50] F.A. Saad, N.M. El-Metwaly, M.S. Refat, A.M. Khedr, Russ. J. Gen. Chem., 88 (2018) 1258–1265.
[51] S. Packiaraj, A. Pushpaveni, S. Govindarajan, J.M. Rawsonc, Cryst. Eng. Comm., 18 (2016) 7978–7993.
[52] A. Pushpaveni, S. Packiaraj, S. Govindarajan, G.T. McCandless, C.F. Fronczek, F.R. Fronczek, Inorg. Chim. Acta, 471 (2018) 537–549.
[53] O.A.M. Ali, J. Therm. Anal. Calorim., 128 (2017) 1579.
[54] M.H. Soliman, G.G. Mohamed, Spectrochim. Acta a, 107(2013) 8.
[55] N. Zare, A. Zabardasti, Appl. Organomet. Chem., 33(2019) e4687.
[56] L.H. Abdel-Rahman, R. M. El-Khatib, L.A.E. Nassr, A. M. Abu-Dief, M. Ismael, A.A. Seleem, Spectrochim. Acta A, 117(2014) 366.
[57] S.A. Aly, J. Radiat. Res. Appl. Sci., 3(2017)163
[58] A. Arunadevi, N. Raman, Appl. Organomet. Chem., 32 (2018) e4250.
[59] Z. Khanam, C.S. Wen, I.U. Bhat, J. King Saud Univ., 27(2015)23.
[60] N.G. Fahad, N.H. Imran, H.A.K. Kyhoiesh, M.K. Al-Hussainawy, Results in Chem., 6, (2023) 101049
[61] S.M. Rida, A.M. Youssef, M.H. Badr, A. Malki, Z.A. Sherif, A.S. Sultan, Arzneimittelforschung, 62 (2012) 63–74.
[62] H.A.K. Kyhoiesh, K.J. Al-Adilee, Inorganica Chim. Acta, 55 (2023) 121598.
[63] H.A.K. Kyhoiesh, K.J. Al-Adilee, Results in Chem.,3 (2021)100245
[64] A. Pushpaveni, S. Packiaraj, S. Poornima, L. Kousalya, S. Govindarajan, Mater. Chem. Phys., 275 (2022) 125213.